Journal of Electroanalytical Chemistry 896 (2021) 115148

Contents lists available at ScienceDirect

Journal of Electroanalytical Chemistry

journal homepage: www.elsevier.com/locate/jelechem

Glutamate adsorption on gold electrodes at different pH values

José M. Gisbert-González [a], Adolfo Ferre-Vilaplana [b,c], Enrique Herrero [a]

[a] Instituto de Electroquímica, Universidad de Alicante, Apdo. 99, E-03080 Alicante, Spain
[b] Instituto Tecnológico de Informática, Ciudad Politécnica de la Innovación, Camino de Vera s/n, E-46022 Valencia, Spain
[c] Departamento de Sistemas Informáticos y Computación, Escuela Politécnica Superior de Alcoy, Universidad Politécnica de Valencia, Plaza Ferrándiz y Carbonell s/n, E-03801 Alcoy, Spain

ARTICLE INFO

Keywords:
Au
Gultamate
Adsorption
Single crystal electrodes

ABSTRACT

Advanced medical applications of gold nanoparticles can use amino acids as surface modifiers. For this reason, understanding the adsorption of amino acids on gold is crucial to improve these applications. Here, the adsorption of glutamate (Glu) on Au(1 0 0) and Au(1 1 0) electrodes has been studied using a combination of electrochemical experiments, and DFT calculations. The adsorption properties have been examined in two different regions, the double layer region, and the OH adsorption/oxide formation region. In the first one, the combined results from the electrochemical experiments and the DFT calculations indicate that Glu is adsorbed in acidic solutions by the two terminal carboxylate groups, each one in a bidentate configuration, and exchanges two electrons upon adsorption. The comparison with the results obtained for the Au(1 1 1) electrode and other molecules containing carboxylic groups confirms this adsorption mode. Glu adsorption also affects the reconstruction process of the Au(1 1 0) and Au(1 0 0) surfaces. On the other hand, in alkaline solutions, glutamate is not adsorbed because the negative charge of the surface prevents its adsorption. In the OH adsorption/oxide formation region, Glu is oxidized when OH is adsorbed, and the results indicate that OH is consumed in this oxidation process. The formation of gold surface oxides inhibits the Glu oxidation reaction.

1. Introduction

Exhibiting a broad diversity of functional groups, and being inherently biocompatible, amino acids have been used as linkers between drugs and metal nanoparticles for targeted drug delivery [1,2], to immobilize biomolecules on electrodes in biosensors [3,4], or as shapers and stabilizers of colloidally synthesized metal nanoparticles in biomedical applications [4]. The role played by the amino acids in these applications is ultimately determined by the specific adsorption behavior of these species on the metal. Thus, the in-depth investigation of the adsorption behavior of amino acids on the main biocompatible metals is essential for the improvement of these applications.

Platinum and gold are among the most studied biocompatible metals for amino acid-modified nanoparticles [5,6]. Despite the topic has been thoroughly investigated for years [7], the knowledge of the adsorption behavior of amino acids on these noble metals is not still complete. Since these interactions depend not only on the nature of the metal but also on the specific geometric arrangement of the surface atoms, to better understand these adsorption processes single crystal surfaces are required. The adsorption behavior of glycine [8,9], L-alanine [10–14], and L-serine [11–15] on single crystals of platinum and gold has been already electrochemically investigated. The consensus would be that these amino acids in solution adsorb on these metals through their carboxylic groups. These adsorption processes, which imply the deprotonation of the carboxylic groups, depend not only on the surface composition and structure but also on the pH and the surface charge of the electrode. The electrochemical behavior of other amino acids, such as tyrosine, tryptophan, methionine, histidine, and cysteine have been also investigated because its redox properties can be used in sensing applications, and diagnosis [16–19].

Having L-glutamic acid (Glu) three groups with acid/base properties (pK_a values of 2.17, 4.25, and 9,67), the main species of Glu in solution depends on the pH. Thus, given that the speciation with the solution pH should influence the adsorption processes, a complete view of the adsorption behavior of Glu from solution has to consider the entire pH range. Combining electrochemical experiments, FTIR spectroscopy, and theoretical DFT calculations, we have recently investigated the adsorption behavior of Glu on the Au(1 1 1) surface at different pH values, following the approach previously used for citrate [20,21]. It was found that Glu bonds to the Au(1 1 1) surface by the two carboxylic groups, exchanging two electrons. Under a similar approach, we cover here the adsorption of Glu on the Au(1 0 0) and Au(1 1 0) surfaces at different pH values, to provide a complete picture of the adsorption behavior of this species on gold in solution. These

E-mail address: herrero@ua.es (E. Herrero)

https://doi.org/10.1016/j.jelechem.2021.115148
Received 9 February 2021; Received in revised form 7 March 2021; Accepted 7 March 2021

results not only provide a better understanding of the adsorption behavior of Glu on gold, facilitating the application of Glu modified gold nanoparticles, but they also help to comprehend the mechanism giving rise to preferentially shaped colloidal nanoparticles of this metal when Glu is used as the growing mediator. Given that it was found in our previous research on the adsorption behavior of Glu on Au(1 1 1) [22] that the specific adsorption of OH at high enough potentials may lead to the oxidation of Glu, the present study is divided into two potential regions: up to 1.2 V vs. RHE, in the so-called double-layer region, and up to 1.7 V vs. RHE (the oxide region). It should be noted that citrate and Glu present a similar structure, with a main chain formed by two terminal carboxylic groups separated by 3 carbon atoms, differing only by their side groups. Whereas citrate has a carboxylic and an OH group in β position, glutamate has only an amino group in the α carbon. The comparison of the adsorption behavior of both species will provide additional knowledge on their adsorption behavior.

2. Methods

2.1. Experimental methods

Clavilier's method was used to prepare the Au(1 0 0) and Au(1 1 0) electrodes [23]. A 0.5 mm diameter gold wire (99.99%) was melted using a small propane-oxygen torch and cooled down slowly to obtain a single crystal bead [24]. This bead was then mounted in a four-cycle goniometer on an optical bench, and oriented in the desired direction using the reflections of a laser beam. Finally, the bead was cut and polished with diamond paste until mirror finishing. Current densities have been normalized using the geometrical area, which, in the case of the single crystal electrodes, coincides with the active area.

The electrochemical experiments were carried out in a glass cell using a reversible hydrogen electrode (RHE) for the pH = 1 and pH = 13 solutions and a $Ag/AgCl_{sat}$ electrode for the pH = 3 and pH = 5 solutions. For data comparison, all the electrode potentials have been converted to the RHE scale. A gold wire was used as counter electrode. Before any experiment, the gold single crystal electrodes were flame annealed and quenched in water, so that the surface arrangement was restored and possible adsorbed species were eliminated [24]. The working solutions were prepared using L(+)-glutamic acid (99% ACROS ORGANICS), perchloric acid (Merck Suprapur®), sodium hydroxide monohydrate (Merck Suprapur®), sodium fluoride (Merck Suprapur®), and ultrapure water (18.2 MΩ·cm, TOC 50 ppb max, Elga Vivendi). Prior to the electrochemical experiments, solutions were deoxygenated with Ar (N50, Air Liquide). Voltammetric experiments were carried out at room temperature using a wave signal generator (EG&G PARC 175), a potentiostat (eDAQ 161), and a digital recorder (eDAQ e-corder 401) workstation.

2.2. Computational methods

All DFT calculations were carried out using numerical basis sets [25], semi-core pseudopotentials [26] (which include scalar relativistic effects), and the revised Perdew-Burke-Ernzerhof (RPBE) [27] functional as implemented in the $Dmol^3$ code [28]. Dispersion forces were corrected by the Tkatchenko and Scheffler method [29]. Continuous solvation effects were taken into account by the conductor-like screening model (COSMO)[30]. The effects of non-zero dipole moments in the supercells were canceled using external fields [31]. Proton-coupled electron transfers were modeled employing the computational hydrogen electrode formalism [32].

The Au(1 0 0) and Au(1 1 0) surfaces were modeled using a big and thick enough periodic supercell for modeling chemisorbed glutamate species with the amino group protonated and deprotonated under neutral total charge conditions. Each model comprises 72 Au atoms (six layers of metal atoms) and a vacuum slab of 20 Å. The most internal 24 Au atoms (two layers of metal atoms) were frozen in their bulk crystal locations, meanwhile, the remaining more external 48 Au atoms were completely relaxed jointly with the adsorbates. The shortest distance between periodic images was in the order of 8.34 and 11.12 Å, for Au(1 0 0) and Au(1 1 0), respectively.

Optimal adsorbent/adsorbate configurations were sought using numerical basis sets of double-numerical quality. For this phase of the calculations, the optimization convergence thresholds were set to 2.0×10^{-5} Ha for the energy, 0.004 Ha/Å for the force, and 0.005 Å for the displacement. The SCF convergence criterion was set to 1.0×10^{-5} Ha for the energy. Assuming the previously optimized configurations, energies were estimated using numerical basis sets of double-numerical quality plus polarization. In this case, the Self Consisted Field (SCF) convergence criterion was set to 1.0×10^{-6} Ha for the energy.

Orbital cutoff radii of 3.1, 3.7, 3.3, and 4.5 Å were always used in the numerical basis set for H, C, O, and Au atoms, respectively. Brillouin zones were always sampled, under the Monkhorst-Pack method using grids corresponding to distances in the reciprocal space of the order of 0.04 1/Å. Convergence was always facilitated by introducing 0.002 Ha of thermal smearing, though total energies were extrapolated to 0 K. The value 78.54 was taken as the dielectric constant for water in the continuous solvation model.

3. Results and discussions

Glu presents three acid/base functional groups, whose pK_a values are 2.17 for the carboxylic group closer to the amino group, 4.25 for the second carboxylic group, and 9.67 for the amino group (Scheme 1). Thus, the main species in solution, the one that should be considered for reactions occurring with Glu, depends on the solution pH. Four different pH regions and four different species should be then considered. At pH < 2.17, the amino group is protonated, giving rise to a cation; in the range of 2.17 < pH < 4.25, the α-carboxyl group deprotonates so that the main solution species is a neutral zwitterion; for 4.25 < pH < 9.67 both carboxylic groups are deprotonated, forming an anion and finally, at pH > 9.67, the amino group loses its acidic proton, yielding an anion with −2 charge. Hence, pH values of 1, 3, 5, and 13, each one in a different region of stability of the Glu species, were selected to study the behavior of Glu on the Au(1 0 0) and Au(1 1 0) surfaces. The supporting electrolytes should comply with two requirements: they should have enough buffer capacity to maintain the solution pH, and the anions should not adsorb specifically on gold to prevent any interference with the Glu adsorption and oxidation processes. The selected solutions in this study were 0.1 M $HClO_4$

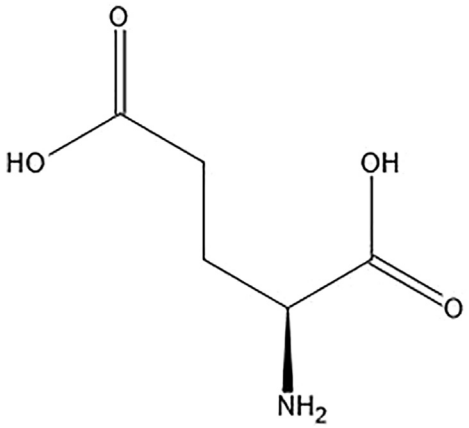

Scheme 1. Glutamic acid structure.

(pH = 1), 2.99 × 10^{-2} M $HClO_4$ + 4.84 × 10^{-2} NaF (pH = 3), 1.70 × 10^{-6} M $HClO_4$ + 10^{-3} M NaF (pH = 5) and 0.1 M NaOH (pH = 13). It should be noted that the combination of $HClO_4$ and NaF gives rise to the formation of the acid-base pair HF/F^-, whose pK_a is 3.17, which allows forming buffered solutions in the pH range between 2 and 5. In fact, the weak interaction between the Au surface and F^- is similar to that of ClO_4^- anions, compensating for the increase in the positive charge density on the electrode surface as the potential is made more positive.

The adsorption behavior of Glu on the considered electrodes is divided into two potential regions: up to 1.2 V, in the so-called double-layer region, and up to 1.7 V (the oxide region). In the first region, Glu species are expected to adsorb, as has been already observed on Au (1 1 1) [22]. In the second region, the specific adsorption of OH and its subsequent oxidation to form surface gold oxides [33–35] may lead to the oxidation of Glu [22]. In any case, the complex behavior of the single crystal surfaces of gold, which are prone to reconstruct, should be taken into account. After the flame-annealing treatment, the Au(1 0 0) surface reconstructs, giving rise to the formation of the (5 × 20) (also terms as (1 0 0)-hex) structure). At potentials below the potential of zero charge (pzc), the reconstruction survives the immersion of the electrode in the solution. However, at E > pzc, the (1 × 1) surface structure recovered, as a result of the lifting of the reconstruction [36–38]. These reconstruction/lifting processes are actually triggered by the surface charge, so that, at potentials above the pcz, the (1 × 1) structure is readily obtained, whereas below the pzc, the most stable surface is the reconstructed one, and it is progressively formed in a slow process [39]. Since the pzc depends on the energetics of the specific surface structure, two different pzc can be measured: for the unreconstructed surface (pzc_u), and for the reconstructed surface (pzc_r). Au(1 1 0) presents an even much more complex behavior, with several possible reconstructed structures, which will be further described below.

3.1. Glu adsorption behavior on Au in the double layer potential region

For the Au(1 0 0) electrode, the voltammetric profiles for the adsorption of Glu at pH values 1, 3, and 5 are displayed in Fig. 1. In the absence of Glu, the voltammetric profile at pH = 1 shows only one peak at ca. 0.85 V in the positive scan direction, which is related to the lifting of the reconstruction of the Au(1 0 0) surface, and a wave above 1.0 V, corresponding to the onset of reversible OH adsorption on the surface (Fig. 1A). In the negative scan direction, there is no peak related to the reconstruction process because this is a very slow process. When Glu is added to the solution, the voltammetric profiles change significantly, even for the lowest Glu concentration. These profiles are similar to those obtained for citrate adsorption [21]. New signals appear in the profile which are due to the Glu adsorption processes. In the positive scan direction, there is a broad wave corresponding to the Glu adsorption process which overlaps with a sharp peak. As before, this peak is related to the lifting of the reconstruction of the Au(1 0 0) surface. As can be seen, the lifting of the reconstruction is triggered by the glutamate-adsorption process (which also alters the surface charge), shifting to more negative potentials when the Glu concentration increases. Adsorbed Glu stabilizes the unreconstructed Au (1 0 0)-(1 × 1) surface, a behavior that is observed when specific adsorption occurs [40]. In the negative scan direction, there is no peak related to the reconstruction because the unreconstructed surface survives until the complete desorption of the adsorbed glutamate.

At pH = 3 (Fig. S1), the voltammetric profiles are very similar to those obtained at pH = 1 solution. In absence of Glu, the peak related to the lifting of the reconstruction is more intense. Additionally, and due to the low ionic strength, there is a minimum in the profile in the negative scan direction which coincides with the pzc_u, according to the Gouy-Chapman theory. When Glu is added to the solution, the only significant difference with the behavior at pH = 1 is the appearance of pairs of reversible peaks at 0.8 V. These peaks might be associated with a potential-induced rearrangement of the adsorbed glutamate. The intensity of these pairs of peaks decreases with the increasing Glu concentration until their complete disappearance (which is even more obvious in the negative swept) probably due to the formation of a more packed structure with the increasing of the Glu concentration. At pH = 5 (Fig. 1B), the upper potential was set at 1.1 V because the Glu oxidation occurs above this potential although the overall behavior is very similar to that already described.

Finally, under alkaline conditions (pH = 13) in the absence of Glu, the voltammogram for the double layer potential region shows the typical peak related to the lifting of reconstruction at 1.0 V (Fig. 1C). The increase in the capacitance has been related to the reorientation of the –OH species before their adsorption [41,42]. After the Glu addition, no changes in the voltammetric profile of the double layer region are observed. This is an indication that Glu species are not adsorbed at pH = 13. Since the pzc_u and pzc_r are located at E > 1.2 V vs. RHE at this pH value (both values are pH-independent in the SHE scale), the surface is negatively charged in the whole potential window shown in Fig. 1C, and thus the interaction of anions with the surface is disfavored. As aforementioned, at this pH value, the main species in solution is the −2 anion. At 1.0 V, a positive current assigned to the Glu oxidation process can be observed. Apparently, it is triggered by the adsorption of the OH process, whose onset is ca. 1.2 V.

For the Au(1 1 0) electrode, the voltammetric profiles for the adsorption of Glu at pH values of 1, 3, and 5 are displayed in Fig. 2. The adsorption behavior of Glu on the Au(1 1 0) surface is even more complex than that observed on Au(1 0 0). To better understand this adsorption behavior, it should be noted that the Au(1 1 0) surface can be also considered as a stepped surface exposing 1 atom-wide terraces with (1 1 1) symmetry separated by (1 1 1) monoatomic steps ((1 1 1)×(1 1 1)) [43,44]. After flame annealing, the Au(1 1 0) surface reconstructs to a (1 × 2) structure, also known as the “missing row” configuration [36]. As for Au(1 0 0), at potentials positive to the pzc this reconstruction lifts exposing the (1 × 1) structure [45,46]. The voltammogram in the supporting electrolyte at pH = 1 shows a broad wave for E > pzc, probably related to the non-specific adsorption processes of the perchlorate/fluoride anions. As the pH is increased, this wave has higher intensity and a second wave at potentials lower than the pzc appears, giving rise to the appearance of a minimum in the vicinity of the pzc.

The addition of Glu to the solution originates voltammetric profiles that are similar to those obtained for citrate [21]. At pH = 1, the profiles have a peak between 0.2 and 0.6 V, and a second process can be observed for E > 0.6 V (Fig. 2A). As expected, these peaks shift to more negative potentials as the Glu concentration increases. At pH = 3, the general behavior is very similar to that described at pH = 1 (Fig. S2). However, at pH = 5, the voltammetric profiles are ill-defined, especially for high Glu concentrations (Fig. 2B). When the Glu adsorption behavior on the Au(1 1 0) surface is compared to that on the Au(1 1 1) [22] and Au(1 0 0) surfaces, a significant difference can be observed. The Glu adsorption processes on the Au(1 1 1) and Au(1 0 0) electrodes increase their potential in the RHE scale as the pH increases. However, the onset of the Glu adsorption on Au (1 1 0) diminishes in the RHE scale. This behavior can be related to the lifting of the reconstruction. At pH = 1, when the electrode is immersed at 0.1 V vs. RHE, the charge is almost zero, starting the lifting of the reconstruction already at this potential. At pH = 5, the potential region under which the reconstructed surface is stable is larger. Since the reconstructed surface can also be considered as a stepped surface consisting of 2 atom-wide (1 1 1) terraces separated by a diatomic (1 1 1) step, the interaction of Glu with this structure is probably different from that with the (1 × 1) structure, and can stabilize it. When the potential increases, the presence of a large coverage of Glu on the surface may lead to the formation of a different surface structure, or to a disordered (1 × 1) surface. Proof of that can

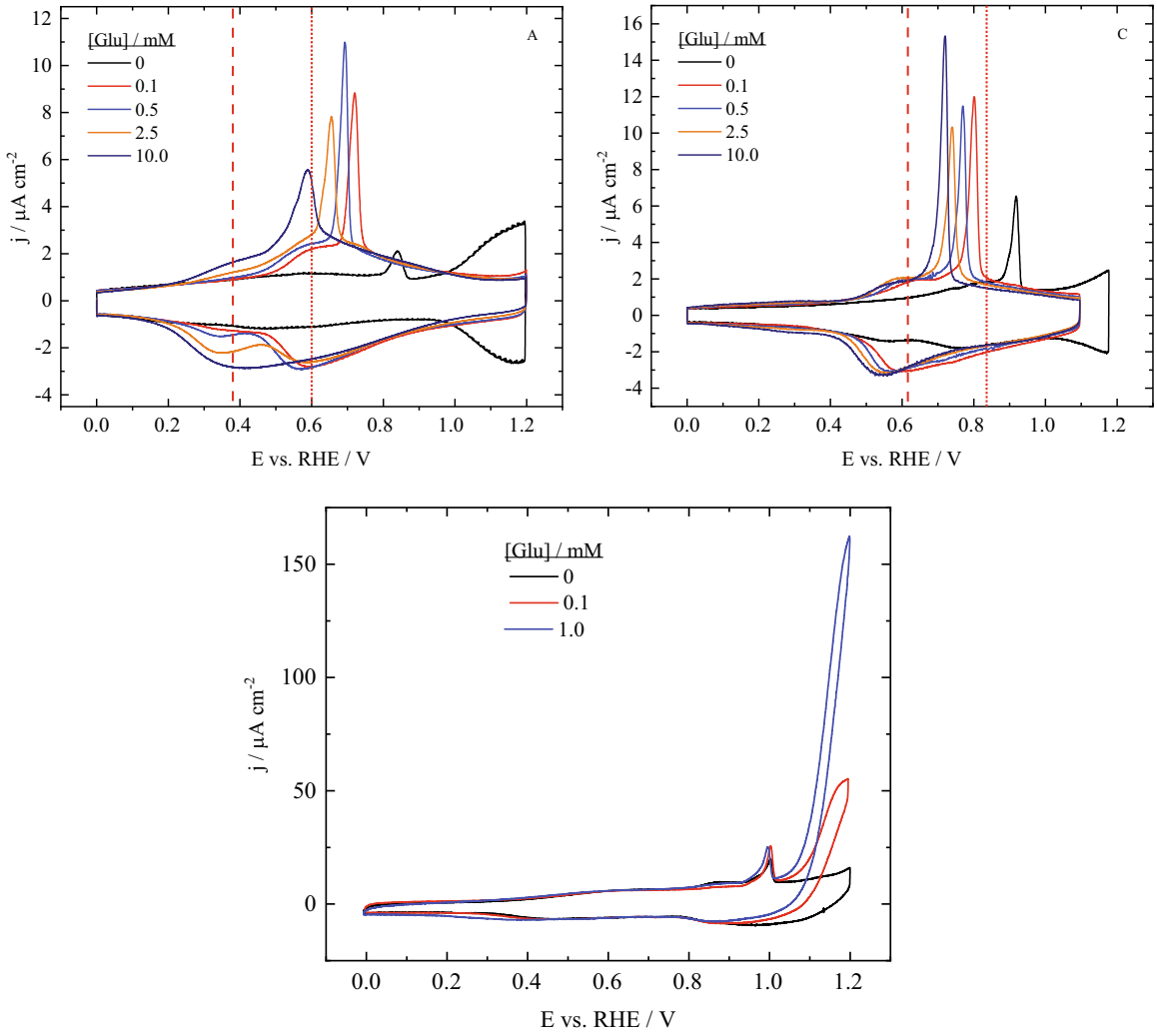

Fig. 1. Voltammetric profiles for Au(1 0 0) with different Glu concentrations in A) 0.1 M $HClO_4$ (pH = 1); B) 1.70 × 10^{-6} M $HClO_4$ + 10^{-3} M NaF (pH = 5) and c) 0.1 M NaOH (pH = 13). Scan rate: 20 mV s^{-1}. The vertical lines mark the position of the pzc_u (dashed line) and pzc_r (dotted line).

be obtained when the electrode potential is kept in the oxide region for some minutes. After the oxide reduction, the voltammogram presents the same characteristics as those observed at lower pH values (Fig. 2C). By keeping high potential values, the surface atoms can rearrange into a lower-energy structure, allowing to reach a well-defined (1 × 1) structure, similar to what is obtained at lower pH values.

In alkaline media (pH = 13), the pzc of the Au(1 1 0) electrode is located at E < 1.2 V. Under these conditions, it could be expected that Glu adsorption could be detected. Nonetheless, the voltammetric profile obtained in the presence of Glu does not differ considerably from that registered in its absence (Fig. 2). On the other hand, some signs of Glu oxidation can be appreciated at the upper potential, in agreement with what is observed for the Au(1 1 1) [22] and Au(1 0 0) electrodes.

Having characterized the adsorption behavior of Glu on gold, adsorbed species and their configurations should be determined. For this purpose, the thermodynamic analysis of the obtained voltammetric profiles on the Au(1 0 0) and Au(1 1 0) surfaces was performed using the procedure described in references [20,21]. Given that this procedure requires that the surface state do not change throughout the selected potential window, only the negative scans of the CVs were considered. In the region of interest of the negative scan direction, it can be considered the surfaces are always in the (1 × 1) structure, because the reconstructions are slow processes, taking place only when Glu has been completely desorbed. To obtain charge density vs. potential curves, the voltammetric profiles displayed in Figs. 1 and 2 have to be integrated, and an integration constant for each curve has to be used. Since Glu is completely desorbed at the low potential limit, and, under these conditions, the surface charge is the same for all the Glu concentrations, a charge value of zero has been assigned as the integration constant for all curves at this potential.

The density charge vs. the potential curves for the Au(1 0 0) and Au (1 1 0) electrodes obtained by integration from the voltammetric profiles of Fig. 1 and Fig. 2 at pH = 5 are displayed in Fig. S3. As happens with the Au(1 1 1) electrode, these curves for lower pH values do not converge in the upper potential limit, and the charge values increase with the Glu concentration at this value. This means either that the adsorption process of Glu has not reached completion, or more probably that Glu is being slowly oxidized at these potentials. Both possibilities prevent any thermodynamic analysis, reason why only the thermodynamic analysis at pH = 5 was carried out.

Gibbs excesses vs. applied potential for the adsorption behavior of Glu on the Au(1 0 0) and Au(1 1 0) electrodes at pH = 5 and 1 mM Glu and their comparison with the corresponding results previously obtained on the Au(1 1 1) electrode [22] are summarized in Fig. 3. It should be highlighted that these excesses include those corresponding to all the possible Glu forms adsorbed on the surface, because the thermodynamic analysis cannot distinguish among them. The Glu adsorption onset on Au(1 1 0) and Au(1 0 0) electrodes is ca. 0.2 V, whereas

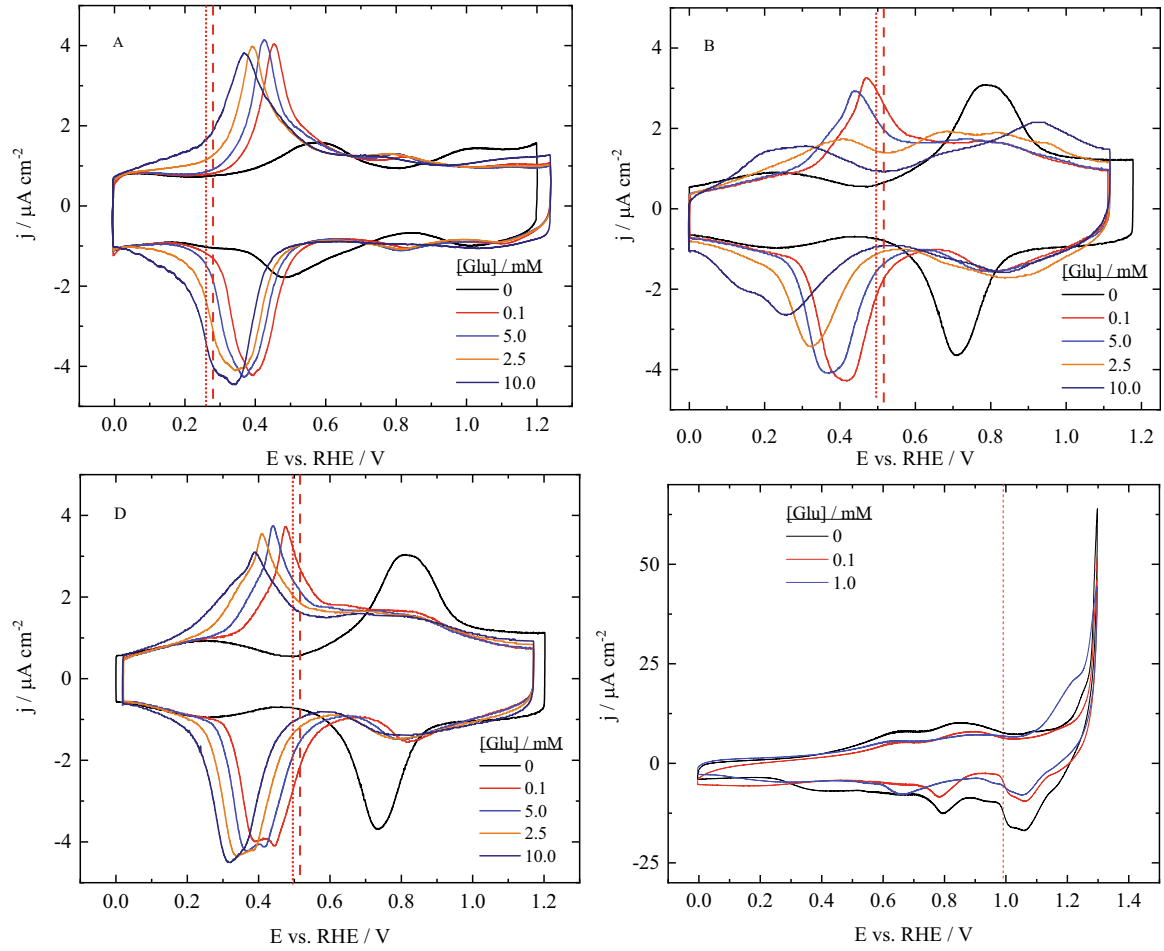

Fig. 2. Voltammetric profiles for Au(1 1 0) with different Glu concentrations in A) 0.1 M $HClO_4$ (pH = 1); B) 1.70 × 10^{-6} M $HClO_4$ + 10^{-3} M NaF (pH = 5) before and (C) after a post-oxidation treatment, and (D) in 0.1 M NaOH (pH = 13). Scan rate 20 mV s^{-1}. The vertical lines mark the position of the pzc_u (dashed line) and pzc_r (dotted line).

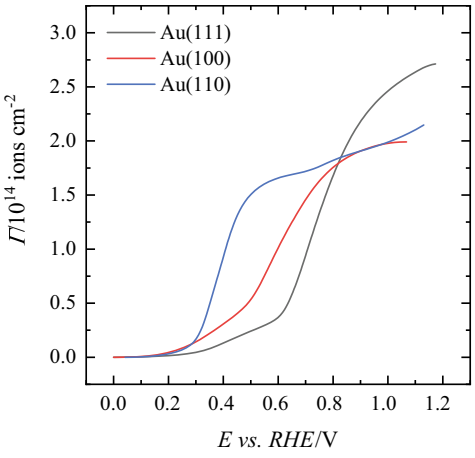

Fig. 3. Gibb excesses for Au(1 0 0), Au(1 1 0) and Au(1 1 1) vs. applied potential in [Glu] = 0.1 M at pH = 5. Data for the Au(1 1 1) electrode was taken from [22].

Glu adlayers are completed at 1.08 and 0.9 V on the Au(1 0 0) and Au (1 1 0) electrodes, respectively. For Au(1 1 0), the curves start to diverge above 1.1 V, probably due to some undetected Glu oxidation. The maximum coverages are 0.17 and 0.22 (2 × 10^{14} and 1.9 × 10^{14} ions cm^{-2}) for the Au(1 0 0) and Au(1 1 0) electrodes, respectively. When these results are compared to those obtained on the Au(1 1 1) surface (2.7 × 10^{14} ions cm^{-2}) [22], it can be concluded that the maximum coverage is higher on this latter electrode, although the adsorption process takes place at higher potentials.

Additional information on the adsorption behavior of Glu on gold can be obtained from the comparison of the voltammetric profiles for the three basal planes of the metal (Fig. 4). Glu adsorption on Au (1 1 0) is the most favorable one. Regarding the Au(1 0 0) and Au (1 1 1) electrodes, there exist differences between the positive and negative voltammogram scan directions. In the positive scan direction, the onsets for Glu adsorption on the Au(1 1 1) and Au(1 0 0) surfaces are very similar. In fact, the lifting of the reconstruction, signaled by the sharp peaks in this scan direction, occurs on both electrodes at almost the same potential, suggesting similar coverages. However, in the negative scan direction, the complete Glu desorption from the Au(1 0 0) electrode takes place at ca. 100 mV more negative potential value than that from the Au(1 1 1) electrode. This effect can be also observed from the excesses (Fig. 3). This dual behavior can be explained also as an effect of the reconstructions. At low potentials, the topmost layer of the reconstructed Au(1 0 0) electrode adopts a hexagonal configuration, which is essentially the same geometry as the one exposed by a perfect (1 1 1) surface. The reconstructed Au(1 1 1) surface presents also a hexagonal structure, though it is slightly compressed in one of the directions with respect to the underlying structure. Thus, on similar geometric arrangements, adsorbed Glu can reach similar geometric

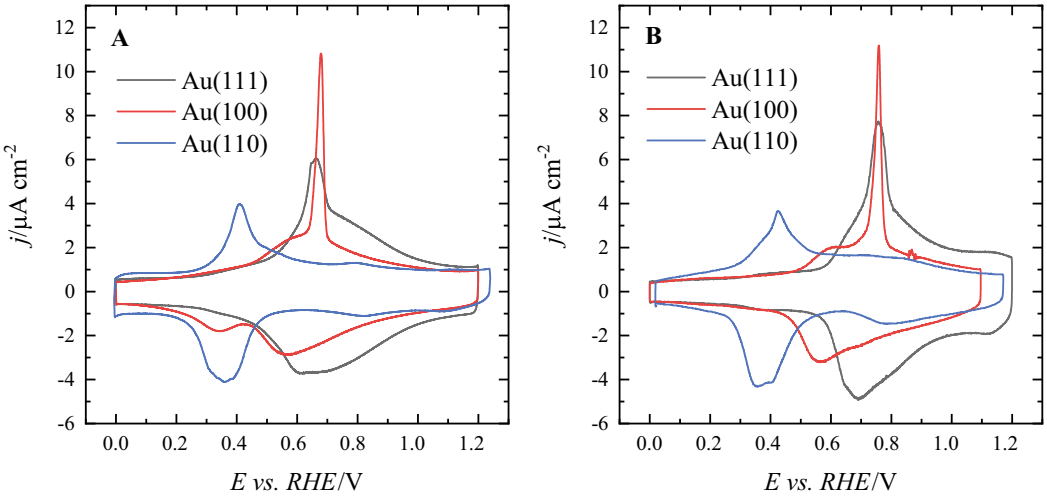

Fig. 4. Comparison of the voltammetric profiles for Au(1 1 1), Au(1 1 0), and Au(1 0 0) in the presence of 0.001 M Glu at A) pH = 1 and B) pH = 5. Scan rate 20 mV s^{-1}.

configurations. Moreover, the pzc_r for both reconstructed surfaces are very close, which indicates that the energetics of the surfaces are also very similar [36,47,48]. As a consequence, similar onsets for the Glu adsorption on both surfaces in the positive scan direction are obtained. Once the reconstruction is lifted, the surface structure and energetics of both surfaces are different, which leads to a different adsorption behavior in the negative scan direction (Fig. 4).

Insights into the species involved in the adsorption processes can be obtained from charge numbers, which provide information on the number of electrons exchanged per adsorbed molecule. Charge numbers can be estimated from the adsorbed surface excesses using the cross differential of the electrocapillary equation [49]:

$$n' = -\frac{1}{F}\left(\frac{\partial\sigma}{\partial\Gamma}\right)_{\mu} = \frac{1}{F}\left(\frac{\partial\mu}{\partial E}\right)_{\sigma} = \frac{RT}{F}\left(\frac{\partial \ln c_{-}}{\partial E}\right)_{\sigma}$$

where n' is the charge number at constant chemical potential, being the reciprocal of the Essin-Markov coefficient. The most reliable charge numbers are those estimated for the potential range where there is a large increase in the excesses with the surface charge or concentration, that is, from 0.2 to 0.8 V for Au(1 0 0), and from 0.2 to 0.6 V for Au (1 1 0). The charge numbers calculated for these potential ranges and the ones previously obtained for Au(1 1 1) [22] are displayed in Fig. 5. As can be observed, these charge numbers for the three electrodes are between 1,5 and 2.5. In fact, in the central region of the considered potential ranges, where the relative errors of the calculations are the smallest, the obtained charge numbers are 1.7, 1.7, and 1.5, for Au(1 1 1), Au(1 0 0), and Au(1 1 0), respectively. Considering that these charge numbers include contributions from double charge processes, it can be proposed that two electrons are exchanged per adsorbed species. Given that at this pH the main species in solution is the anion with a −1 charge, the proposed adsorption reaction is:

$$^{-}OOC\text{ - }(CH_2)_2\text{ - }CH(NH_3^{+})\text{ - }COO^{-}$$
$$+\,2Au \rightleftharpoons Au\text{ - }OOC\text{ - }(CH_2)_2\text{ - }CH(NH_3^{+})\text{ - }COO\text{ - }Au + 2e^{-}$$

This result suggests that, on the three basal planes of gold, Glu adsorbs through both carboxylate groups.

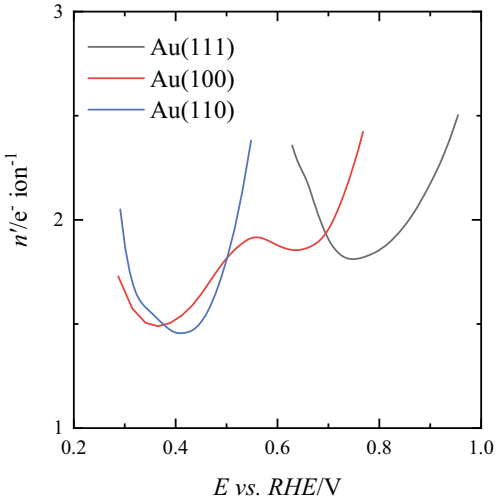

Fig. 5. Charge number vs. applied potential for [Glu] = 0.001 M at pH = 5 for the gold single crystal electrodes. Data for the Au(111) has been obtained from [22].

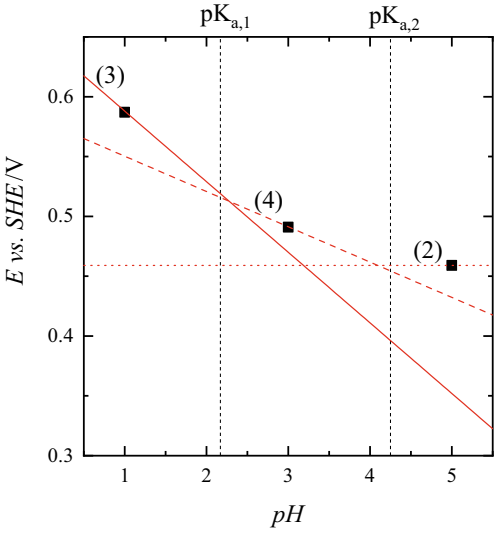

Fig. 6. Potential in the SHE scale of the peak associated with the lifting of the reconstruction of Au(1 0 0) for [Glu] = 0.001 M vs. pH. The red lines display the expected trends of the peak potential according to the reactions (the numbers in brackets correspond to the equations in the text). The vertical lines mark the positions of the pK_a values.

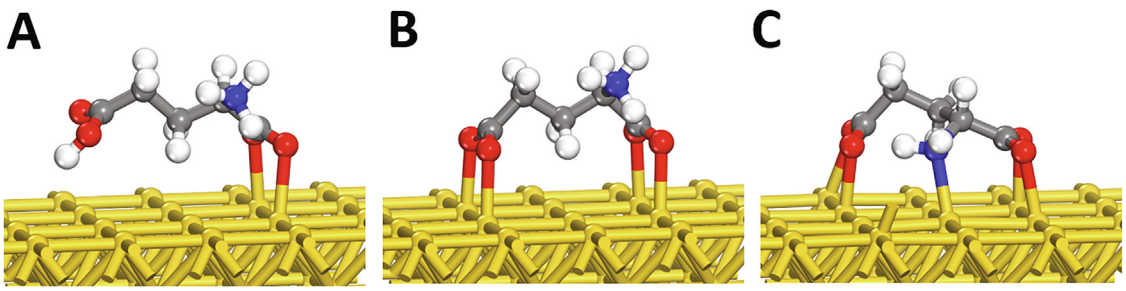

Fig. 7. Glu adsorbed configurations on the Au(1 0 0) surface under neutral total charge conditions with the protonated (A and B) and deprotonated (C) amine group and attached to the surface by one (A) and two (B and C) dehydrogenated carboxylic groups in the bidentate configuration.

Table 1
Energetics (ΔG/eV) of the adsorption processes of Glu on the three basal planes of gold for the different configurations of Fig. 7.

	ΔG/eV		
Conf.	Au(1 0 0)	Au(1 1 0)	Au(1 1 1)
A	−1.24	−0.60	−0.67
B	−0.81	−0.57	0.01
C	−0.58	0.29	0.55

Additional pieces of evidence that Glu is adsorbed through the two carboxylate groups on the three basal planes of gold can be obtained by studying the pH dependence of these adsorption processes. The proposed reaction takes place into the pH range between pK_{a2} and pK_{a3}. Thus, considering that the main Glu species in solution depends on the pH, when $pH < pK_{a1}$, the proposed reaction is:

$$HOOC - (CH_2)_2 - CH(NH_3^+) - COOH + 2Au \rightleftharpoons Au - OOC - (CH_2)_2 - CH(NH_3^+) - COO - Au + 2H^+ + 2e^-$$

whereas, for $pK_{a1} < pH < pK_{a2}$, the proposed reaction transforms into

$$HOOC - (CH_2)_2 - CH(NH_3^+) - COO^- + 2Au \rightleftharpoons Au - OOC - (CH_2)_2 - CH(NH_3^+) - COO - Au + H^+ + 2e^- \quad (4)$$

These two reactions give rise to different potential vs. solution pH slopes for the Glu adsorption processes. In the SHE scale, the adsorption process should shift 59 mV per pH unit in the region where $pH < pK_{a1}$, whereas 29 mV and 0 mV per pH unit are expected in the other two regions, respectively. The Glu adsorption process on the Au(1 1 1) electrode follows these slopes [22]. And, as can be

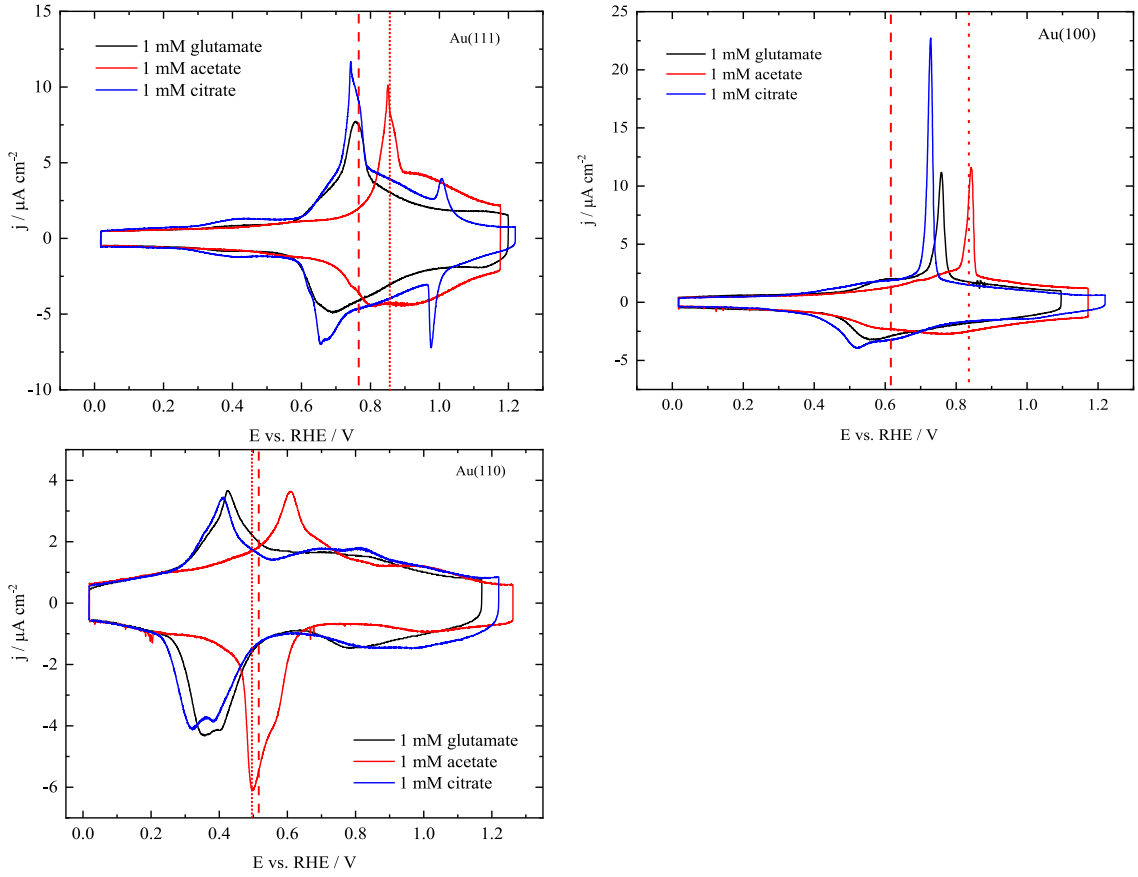

Fig. 8. Voltammetric profiles for the adsorption of 1 mM Glu, acetate, and citrate at pH = 5 on the three basal-planes gold. The vertical lines mark the position of the pzc_u (dashed line) and pzc_r (dotted line).

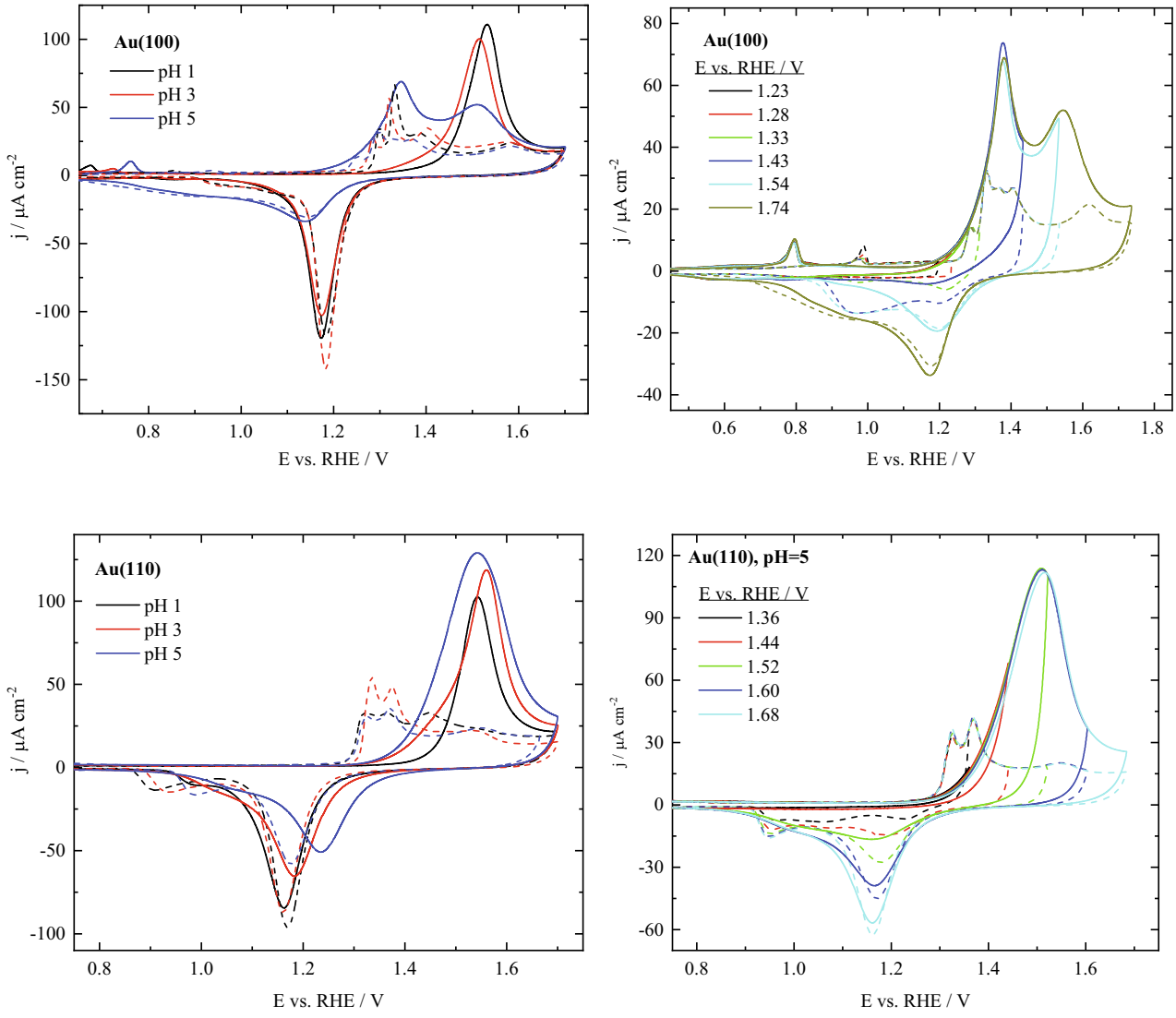

Fig. 9. Voltammetric profiles for the Au(1 0 0)and Au(1 1 0) electrodes in the presence (full lines) and absence (dashed lines) of 1 mM Glu under acidic conditions for the oxide potential region. Scan rate 20 mV s^{-1}.

observed in Fig. 4, the overall shift of the Glu adsorption processes with pH on the Au(1 0 0) and Au(1 1 0) electrodes is the same as that observed for Au(1 1 1), which would confirm that the three adsorption processes would be essentially the same. Additionally, a semi-quantitative analysis of the shift can be carried out by using a prominent feature of the obtained voltammograms. Assuming that the peak related to the lifting of the Au(1 0 0) reconstruction occurs at constant Glu coverage, they can be plotted in the SHE scale together with the different trend lines reflecting the expected potential change of the peak in each pH region. As can be seen (Fig. 6), these lines intersect, within the error of the experiments, at the pKa values, which validates the proposed mechanism.

To verify the conclusions reached from the experiments, plausible configurations of Glu species adsorbed on the three basal planes of gold were examined using DFT calculations. For each relevant configuration obtained under total neutral charge conditions the free energy of the corresponding adsorption process was estimated using the energy of the corresponding surface and that of a hydrated glutamic acid molecule as the reference, and adjusting the stoichiometry of the processes with the required number of H_2 molecules. It was found that, on each basal plane, Glu can be adsorbed on the surface through one and two dehydrogenated carboxylic groups in the bidentate configuration (Fig. 7A and B) with the amino group protonated. Additionally, the protonated amino group can be deprotonated and bonded to the surface (Fig. 10C). The free energies corresponding to all these adsorption processes on the three basal planes of gold are summarized in Table 1. As can be seen, the Glu adsorption through its two deprotonated carboxylic groups in bidentate configuration (Fig. 10B) is a favorable enough process involving the transfer of two electrons, which is consistent with the charge numbers derived from the experiments (Fig. 5). Additionally, the energy values summarized in Table 1 also indicate that the order of the adsorption strength of Glu on the three basal planes of gold is Au(1 1 0) > Au(1 0 0) > Au(1 1 1), which is also in agreement with the experiments (Fig. 3). It should be highlighted that, in the absence of dispersion forces, the calculations indicate that Glu would be adsorbed on gold through a single dehydrogenated carboxylic group in bidentate configuration with the main chain perpendicular to the surface. From this configuration, the bonding to the surface by the second carboxylic group would originate structural tension resulting in an unfavorable process. This configuration would be not consistent with the experiments. However, when dispersion forces are included in the calculations, the configuration in which Glu is adsorbed through a single deprotonated carboxylic group in the bidentate configuration leans towards the surface

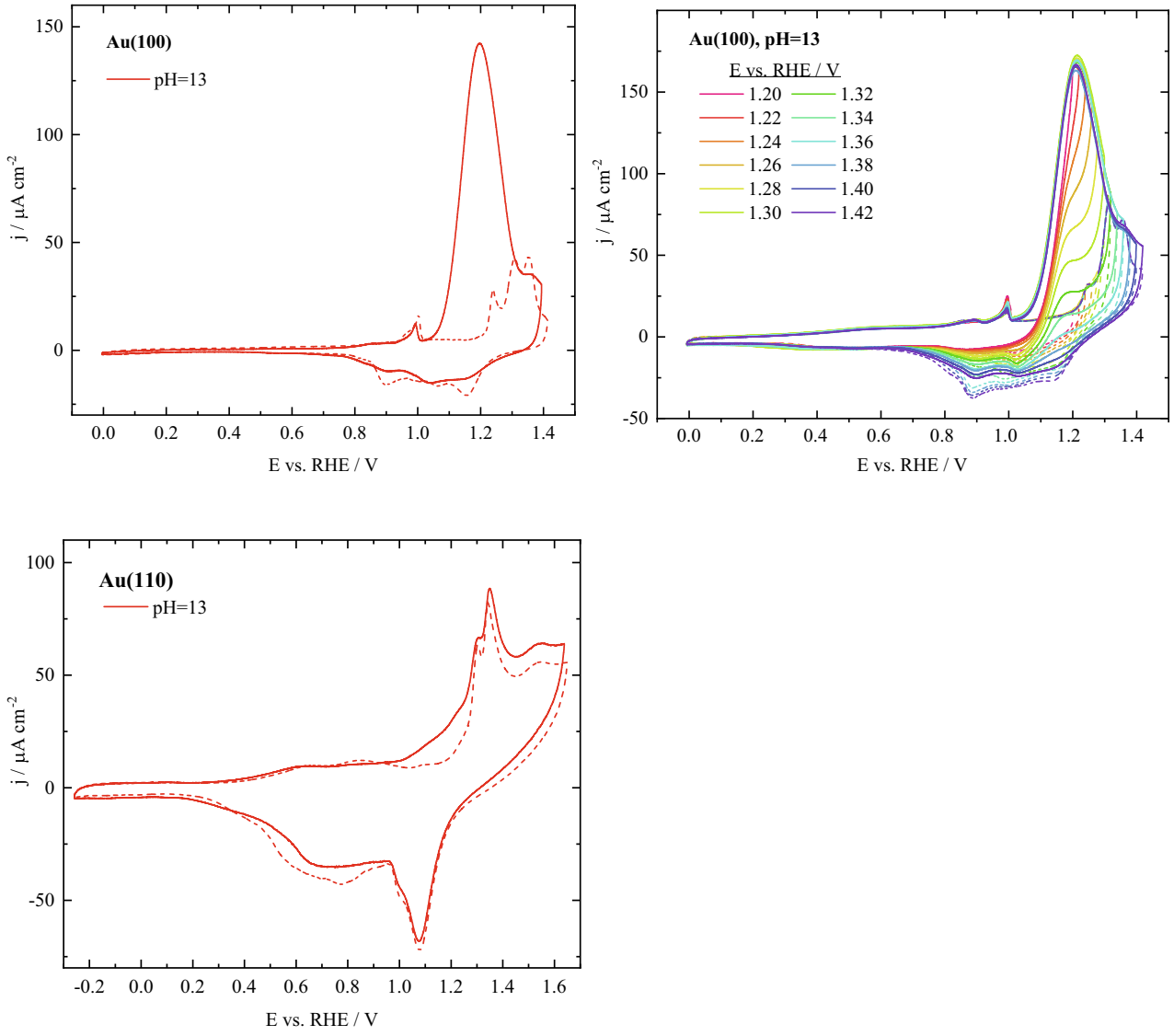

Fig. 10. Voltammetric profiles for the Au(1 0 0) and Au(1 1 0) electrodes in the presence (full lines) and absence(dashed lines) of 1 mM at pH = 5 and pH = 13 for the oxide potential region under different upper potential limits. Scan rate 20 mV s^{-1}.

(Fig. 7A). From configuration in which the main chain is almost parallel to the surface, the evolution to the configuration shown in Fig. 7B is a much more favorable process. Thus, dispersion forces are essential to sufficiently capture the interaction of Glu with these surfaces.

The comparison of the adsorbed behavior of Glu on gold with that obtained with other molecules having carboxylic groups provides further pieces of evidence of the adsorption of Glu through their deprotonated carboxylic groups in the bidentate configuration. Acetic acid, which contains only one carboxylic group, and citric acid, which has three carboxylic groups, were selected for comparison. Acetate is adsorbed on gold through its single carboxylate group in the bidentate configuration on the basal planes [50]. Citrate is adsorbed on gold through its two terminal carboxylate groups in the bidentate configuration on Au(1 0 0), Au(1 1 1), and Au(1 1 0) [21]. Geometric restrictions prevent its adsorption through the third carboxylate group except on Au(1 1 1), on which this adsorption configuration is attained at high potentials [21]. As can be seen in Fig. 8, adsorption of acetate takes place on the three electrodes at higher potentials values, whereas for Glu and citrate, adsorption potentials are almost the same. In fact, for these two species, the voltammetric profiles are very similar in shape and potentials, highlighting parallel adsorption behavior. The higher adsorption potentials for acetate can be easily justified because it is adsorbed by one carboxylate group, whereas additional carboxylate groups are involved in the adsorption of the other molecules, increasing the adsorption energy. The similar behavior of citrate and Glu is a consequence of the similar molecular structure and provides a clear indication that both adsorption processes involve the same groups attached to the surface, that is, both species are attached to the surface by their two terminal carboxylate groups. The only significant difference between Glu and citrate adsorption on gold is observed for the Au(1 1 1) electrode. In this case, although the potentials and overall shape of the voltammograms are also similar, the total charge for citric acid is higher, which would indicate that the third carboxylate group is also involved in the adsorption process, exchanging one additional electron, as has been proposed [21]. However, due to the geometric constraints, the additional attachment of citrate to the surface would not increase the adsorption energy, having the voltammograms the same shape.

3.2. Behavior of adsorbed Glu on gold in the oxide potential region

The results in the region up to 1.2 V show that, at this upper potential limit, the oxidation of Glu is taking place. The oxidation appears to be related to the adsorption of OH on the surface. For this reason, the

voltammetric scan was extended in the oxide region. Fig. 9 shows the voltammetric profiles for the Au(1 0 0) and Au(1 1 0) electrodes in the presence and absence of 1 mM Glu under acidic conditions in the potential region up to 1.7 V. As can be seen, the presence of Glu, which is strongly adsorbed at E < 1.2 V, retards the adsorption of OH on the surface because the peaks in this region in absence of Glu disappear when Glu is added. However, at potentials above 1.4 V, a significant oxidation wave related to Glu oxidation can be observed. This oxidation is completely inhibited at the upper potential limit. For this oxidation process, the onset is displaced at lower potentials as the solution pH increases. This can be even better observed for the Au(1 0 0) electrode at pH = 5, where the oxidation onset is ca. 1.2 V. This effect can be related to the Glu adsorption strength. As the pH increases, the electrode charge at 1.2 V vs. RHE becomes less positive, and thus, the Glu adsorption becomes less strong. Under these conditions, adsorbed OH, which triggers Glu oxidation, can more easily replace previously adsorbed Glu species, leading to Glu oxidation. On the other hand, the oxidation currents diminish after the peaks at ca. 1.4 and 1.5 V for Au(1 0 0) and Au(1 1 0), respectively. This diminution seems to be related to the transformation of adsorbed OH into adsorbed O, that is, the formation of a surface oxide layer [33]. In fact, no oxidation currents are detected in the negative scan direction, and the peak related to the reduction of the surface oxides has almost the same charge as that measured in the absence of Glu. Then, the surface state in the upper potential limit and that observed in the absence of Glu are almost the same.

These results indicate that adsorbed OH catalyzes the oxidation of Glu, whereas the formation of a surface oxide acts as an inhibitor. To further analyze these roles, a series of voltammograms with different upper potential limits were recorded and analyzed (Fig. 9). When the upper potential limit is close to 1.3 V, the oxidative currents in the positive and negative scan directions are almost the same, and unlike the profile in absence of Glu, no sign of the desorption of OH can be observed in the negative scan direction. Only when the upper potential limit is above 1.4 and 1.5 V for the Au(1 0 0) and Au(1 1 0) surfaces, respectively, the oxidative currents in the negative scan direction are significantly smaller than those recorded in the positive scan direction. Moreover, the charge for OH desorption is significantly smaller. This fact indicates that not only adsorbed OH is catalyzing Glu oxidation, but also that adsorbed OH is being consumed in this process. Also, the reduction peak for the oxides in the negative scan direction is only restored when the upper potential limit is above 1.5 and 1.6 V for the Au(1 0 0) and Au(1 1 0) electrodes, respectively. At these potential values, the surface oxides are readily formed.

Under alkaline conditions, the behavior for the Au(1 0 0) electrode is similar to that observed in acidic solutions (Fig. 10). The only significant difference is that the onset for the oxidation of Glu species takes place at lower potential values, as expected, since Glu is not adsorbed in this medium. As happens in acidic solutions, adsorbed OH is also involved in the Glu oxidation reaction. On the other hand, on the Au (1 1 0) electrode, Glu oxidation is almost negligible. Adsorbed OH does not facilitate the oxidation of Glu on Au(1 1 0), because, on this surface, these co-adsorbates are not adsorbed in a configuration that is favorable for their interaction leading to Glu oxidation.

4. Conclusions

Glu adsorption on gold single crystal electrodes at different pH values has been here characterized using a combination of electrochemical experiments and DFT calculations. The comparison with the behavior of other molecules containing carboxylic groups also has provided insight into the adsorption mechanism. The results indicate that, in the double layer potential region and under acidic conditions, glutamate adsorbs in a positively charged surface by its two terminal carboxylate groups, each one of them in the bidentate configuration. These groups dehydrogenate upon adsorption, exchanging two electrons. In alkaline media, since the surface charge is negative in this potential region, Glu is not adsorbed. On the other hand, the adsorption of OH on the surface is a requirement for the oxidation of Glu. This oxidation process is inhibited when the OH adsorbed layer transforms into an oxide layer.

Declaration of Competing Interest

The authors declare that they have no known competing financial interests or personal relationships that could have appeared to influence the work reported in this paper.

Acknowledgment

Financial support from Ministerio de Ciencia e Innovación (Project PID2019-105653GB-100) and Generalitat Valenciana (Project PROMETEO/2020/063) is acknowledged.

Appendix A. Supplementary data

Supplementary data to this article can be found online at https://doi.org/10.1016/j.jelechem.2021.115148.

References

[1] P.S. Ghosh, C. Kim, G. Han, N.S. Forbes, V.M. Rotello, Efficient gene delivery vectors by tuning the surface charge density of amino acid-functionalized gold nanoparticles, ACS Nano 2 (2008) 2213–2218.
[2] E.C. Dreaden, A.L. Alkilany, X. Huang, C.J. Murphy, M.A. El-Sayed, The golden age: Gold nanoparticles for biomedicine, Chem. Soc. Rev. 41 (2012) 2740–2779.
[3] D.C. Goldstein, P. Thordarson, J.R. Peterson, The bioconjugation of redox proteins to novel electrode materials, Aust. J. Chem. 62 (2009) 1320–1327.
[4] K. Hernandez, R. Fernandez-Lafuente, Control of protein immobilization: Coupling immobilization and site-directed mutagenesis to improve biocatalyst or biosensor performance, Enzyme Microb. Technol. 48 (2011) 107–122.
[5] D. Pedone, M. Moglianetti, E. De Luca, G. Bardi, P.P. Pompa, Platinum nanoparticles in nanobiomedicine, Chem. Soc. Rev. 46 (2017) 4951–4975.
[6] R. Shukla, M. Chaudhary, A. Basu, R.R. Bhonde, M. Sastry, Biocompatibility of gold nanoparticles and their endocytotic fate inside the cellular compartment: A microscopic overview, Langmuir 21 (2005) 10644–10654.
[7] O. Yamauchi, A. Odani, M. Takani, Metal–amino acid chemistry. Weak interactions and related functions of side chain groups, J. Chem. Soc. - Dalton Trans. (2002) 3411–3421.
[8] F. Huerta, E. Morallon, F. Cases, A. Rodes, J.L. Vázquez, A. Aldaz, Electrochemical behaviour of amino acids on pt(h, k, l): A voltammetric and in situ ftir study.1. Glycine on pt(111), J. Electroanal. Chem. 421 (1997) 179–185.
[9] F. Huerta, E. Morallon, J.L. Vázquez, J.M. Pérez, A. Aldaz, Electrochemical-behavior of amino-acids on pt(hkl) - a voltammetric and in-situ ftir study - part iii - glycine on pt(100) and pt(110), J. Electroanal. Chem. 445 (1998) 155–164.
[10] L. Ruan, H. Ramezani-Dakhel, C.-Y. Chiu, E. Zhu, Y. Li, H. Heinz, Y. Huang, Tailoring molecular specificity toward a crystal facet: A lesson from biorecognition toward pt{111}, Nano Lett. 13 (2013) 840–846.
[11] A.P. Sandoval, J.M. Orts, A. Rodes, J.M. Feliu, A comparative study of the adsorption and oxidation of l-alanine and l-serine on au(100), au(111) and gold thin film electrodes in acid media, Electrochim. Acta 89 (2013) 72–83.
[12] F. Huerta, E. Morallon, J.L. Vazquez, A. Aldaz, Electrochemical behaviour of amino acids on pt(hkl). A voltammetric and in situ ftir study part iv. Serine and alanine on pt(100) and pt(110), J. Electroanal. Chem. 475 (1999) 38–45.
[13] F. Huerta, E. Morallon, F. Cases, A. Rodes, J.L. Vázquez, A. Aldaz, Electrochemical-behavior of amino-acids on pt(h, k, l) - a voltammetric and in-situ ftir study.2. Serine and alanine on pt(111), J. Electroanal. Chem. 431 (1997) 269–275.
[14] A.P. Sandoval, J.M. Orts, A. Rodes, J.M. Feliu, Dft and in situ infrared studies on adsorption and oxidation of glycine, l-alanine, and l-serine on gold electrodes, in: A. Wieckowski, C. Korzeniewski, B. Braunschweig (Eds.), Wiley ser electrocat, John Wiley & Sons, Inc., 2013, pp. 241–265.
[15] G. Horanyi, A direct and indirect radiotracer study of the adsorption of serine at a platinized platinum electrode, J. Electroanal. Chem. 304 (1991) 211–217.
[16] A.H.B. Dourado, F.C. Pastrián, S.I.C.D. Torresi, The long and successful journey of electrochemically active amino acids. From fundamental adsorption studies to potential surface engineering tools, Anais da Academia Brasileira de Ciências 90 (2018) 607–630.
[17] A.H.B. Dourado, A.P. de Lima Batista, A.G.S. Oliveira-Filho, P.T.A. Sumodjo, S.I. Cordoba de Torresi, L-cysteine electrooxidation in alkaline and acidic media: A combined spectroelectrochemical and computational study, RSC Adv. 7 (2017) 7492–7501.

[18] A.M. Oliveira-Brett, V.C. Diculescu, T.A. Enache, I.P.G. Fernandes, A.-M. Chiorcea-Paquim, S.C.B. Oliveira, Bioelectrochemistry for sensing amino acids, peptides, proteins and DNA interactions, Curr. Opin. Electrochem. 14 (2019) 173–179.
[19] E. Paleček, J. Tkáč, M. Bartošík, T. Bertók, V. Ostatná, J. Paleček, Electrochemistry of nonconjugated proteins and glycoproteins. Toward sensors for biomedicine and glycomics, Chem. Rev. 115 (2015) 2045–2108.
[20] J.M. Gisbert-Gonzalez, J.M. Feliu, A. Ferre-Vilaplana, E. Herrero, Why citrate shapes tetrahedral and octahedral colloidal platinum nanoparticles in water, J. Phys. Chem. C 122 (2018) 19004–19014.
[21] J.M. Gisbert-Gonzalez, W. Cheuquepán, A. Ferré-Vilaplana, J.M. Feliu, E. Herrero, Citrate adsorption on gold: Understanding the shaping mechanism of nanoparticles, J. Electroanal. Chem. 875 (2020) 114015.
[22] J.M. Gisbert-González, W. Cheuquepán, A. Ferre-Vilaplana, E. Herrero, J.M. Feliu, Glutamate adsorption on the au(111) surface at different ph values, J. Electroanal. Chem. 880 (2021) 114870.
[23] J. Clavilier, R. Faure, G. Guinet, R. Durand, Preparation of monocrystalline pt microelectrodes and electrochemical study of the plane surfaces cut in the direction of the 111 and 110 planes, J. Electroanal. Chem. 107 (1980) 205–209.
[24] A. Rodes, E. Herrero, J.M. Feliu, A. Aldaz, Structure sensitivity of irreversibly adsorbed tin on gold single-crystal electrodes in acid media, J. Chem. Soc. Faraday T. 92 (1996) 3769–3776.
[25] B. Delley, An all-electron numerical method for solving the local density functional for polyatomic molecules, J. Chem. Phys. 92 (1990) 508–517.
[26] B. Delley, Hardness conserving semilocal pseudopotentials, Phys. Rev. B 66 (2002) 155125.
[27] B. Hammer, L.B. Hansen, J.K. Nørskov, Improved adsorption energetics within density-functional theory using revised perdew-burke-ernzerhof functionals, Phys. Rev. B 59 (1999) 7413–7421.
[28] B. Delley, From molecules to solids with the dmol(3) approach, J. Chem. Phys. 113 (2000) 7756–7764.
[29] A. Tkatchenko, M. Scheffler, Accurate molecular van der waals interactions from ground-state electron density and free-atom reference data, Phys. Rev. Lett. 102 (2009) 073005.
[30] B. Delley, The conductor-like screening model for polymers and surfaces, Mol. Simulat. 32 (2006) 117–123.
[31] J. Neugebauer, M. Scheffler, Adsorbate-substrate and adsorbate-adsorbate interactions of na and k adlayers on al(111), Phys. Rev. B 46 (1992) 16067–16080.
[32] J.K. Nørskov, J. Rossmeisl, A. Logadottir, L. Lindqvist, J.R. Kitchin, T. Bligaard, H. Jónsson, Origin of the overpotential for oxygen reduction at a fuel-cell cathode, J. Phys. Chem. B 108 (2004) 17886–17892.
[33] H. Angerstein-Kozlowska, B.E. Conway, A. Hamelin, L. Stoicoviciu, Elementary steps of electrochemical oxidation of single-crystal planes of au.1. Chemical basis of processes involving geometry of anions and the electrode surfaces, Electrochim. Acta 31 (1986) 1051–1061.
[34] A. Hamelin, The crystallographic orientation of gold surfaces at the gold-aqueous solution interphaces, J. Electroanal. Chem. 142 (1982) 299.
[35] H. Angersteinkozlowska, B.E. Conway, A. Hamelin, L. Stoicoviciu, Elementary steps of electrochemical oxidation of single-crystal planes of au.2. A chemical and structural basis of oxidation of the (111) plane, J. Electroanal. Chem. 228 (1987) 429–453.
[36] D.M. Kolb, J. Schneider, Surface reconstuction in electrochemistry: Au(100)-(5x20), au(111)-(1x23) and au(110)-(1x2), Electrochim. Acta 31 (1986) 929–936.
[37] M.A. Van Hove, R.J. Koestner, P.C. Stair, J.P. Biberian, L.L. Kesmodel, I. Bartos, G. A. Somorjai, The surface reconstructions of the (100) crystal faces of iridium, platinum, and gold: I. Experimental observations and possible structural models, Surf. Sci. 103 (1981) 189–217.
[38] X. Gao, A. Hamelin, J.M. Weaver, Potential-dependent reconstruction at ordered au(100)-aqueous interfaces as probed by atomic-resolution scanning tunneling microscopy, Phys. Rev. Lett. 67 (1991) 618–621.
[39] X. Gao, S.C. Chang, X. Jiang, A. Hamelin, M.J. Weaver, Emergence of atomic level structural information for oredered metal-solution interfaces : Some recent contributions from in- situ infrared spectroscopy and scanning tunneling microscopy, J. Vac. Sci. Technol., A 10 (1992) 2972.
[40] D.M. Kolb, J. Schneider, The study of reconstructed electrode surfaces: Au(100)-(5x20), Surf. Sci. 162 (1985) 764–775.
[41] S. Strbac, A. Hamelin, R.R. Adzic, Electrochemical indication of surface reconstruction of (100), (311) and (111) gold faces in alkaline solutions, J. Electroanal. Chem. 362 (1993) 47–53.
[42] A. Hamelin, M.J. Sottomayor, F. Silva, S.C. Chang, M.J. Weaver, Cyclic voltammetric characterization of oriented monocrystalline gold surfaces in aqueous alkaline-solution, J. Electroanal. Chem. 295 (1990) 291–300.
[43] G. Binnig, H. Rohrer, G. Ch., E. Weibel, (111) facets as the origin of reconstructed au(110) surfaces, Surf. Sci. Lett., 131 (1983) L379-L384.
[44] X. Gao, A. hamelin, J.M. Weaver, Reconstruction at ordered au(110)-aqueous interfaces as probed by atomic-resolution scanning tunneling microscopy, Phys. Rev. B – Conden. Matt. Mater. Phys. 44 (1991) 10983–10986.
[45] A. Hamelin, Note on the behavior of the (111) gold face in electrolytic solutions, J. Electroanal. Chem. 210 (1986) 303–309.
[46] A. Hamelin, Study of the (210) face of gold in aqueous solutions, J. Electroanal. Chem. 138 (1982) 395–400.
[47] U.W. Hamm, D. Kramer, R.S. Zhai, D.M. Kolb, The pzc of au(111) and pt(111) in a perchloric acid solution: An ex situ approach to the immersion technique, J. Electroanal. Chem. 414 (1996) 85–89.
[48] X. Gao, A. Hamelin, M.J. Weaver, Atomic relaxation at ordered electrode surfaces probed by scanning tunneling microscopy: Au(111) in aqueous solution compared with ultrahigh-vacuum environments, J. Chem. Phys. 95 (1991) 6993–6996.
[49] R.P.S. Trasatti, Interphases in systems of conducting phases, J. Electroanal. Chem. 205 (1986) 359–376.
[50] A. Berna, J.M. Delgado, J.M. Orts, A. Rodes, J.M. Feliu, Spectroelectrochemical study of the adsorption of acetate anions at gold single crystal and thin-film electrodes, Electrochim. Acta 53 (2008) 2309–2321.